SIZE EFFECT IN PENETRATION OF SEA ICE PLATE WITH PART-THROUGH CRACKS. II: RESULTS

By Zdeněk P. Bažant,[1] Fellow, ASCE, and Jang Jay H. Kim[2]

ABSTRACT: After development of the theory in the part I paper, systems of up to 300 nonlinear equations are solved in this paper by the Levenberg-Marquardt optimization algorithm. The maximum load is reached when the circumferential cracks begin to form. Numerical calculations show a typical quasi brittle size effect such that the plot of log σ_N versus log h (where α_N = nominal stress at maximum load and h = plate thickness) is a descending curve whose slope is negligible only for $h < 0.2$ m and then gets gradually steeper, asymptotically approaching $-1/2$. The calculated size effect agrees with the existing test data, and contradicts previous plasticity solutions.

INTRODUCTION

The part I paper (Bažant and Kim 1998) in this issue presented the theory of a numerical solution of the fracture problem of penetration of an object through a floating ice plate. The present paper will use the theory to obtain results on the size effect and compare them to experimental data. Broader issues of scaling will also be studied. All the notations and definitions from the part I paper will be retained.

NUMERICAL CALCULATION OF DEFLECTION, STRESS, AND CRACK DEPTH PROFILES

To study the vertical depth profile of the radial crack, the stress distributions and, most important, the size effect, ice plates with various thicknesses are analyzed numerically. The schematic picture of the part-through numerical analysis model of an ice plate is shown in Figs. 1 and 2 of part I. An ice plate with an angle of 60° between the radial cracks in a star pattern is chosen as the basic case to solve. This is the angle that was commonly observed in the field tests by Frankenstein (1963). Although his experiments were carried out on lake ice, it seems reasonable to assume that the wedge angle would be the same for sea ice.

Because the structure is symmetric with respect to any crack line and the centerline of any wedge, one needs to analyze only a half wedge, with a 30° central angle. The ice plate is assumed to have a fixed support on a circle of radius $3L$. This support is far enough from the applied load resultant to ensure that the region with the crack behaves almost as if the plate were infinite.

The vertical load is considered to be applied on the plate as a uniformly distributed load along the edge of a circular hole of radius $0.1L$, where L is the flexural wavelength of ice. This is done for the sake of convenience, to avoid dealing with the moment singularity that would occur if the load were concentrated. The behavior at the beginning of crack propagation is of course affected by the presence of the hole, but at radial distances that matter for the long crack at maximum load (which exceeds $0.2L$ for all L), the behavior is nearly the same as for a plate in which the load is either concentrated or applied uniformly over the area of the circle. This fact (which is a manifestation of the Saint-Venant principle) justifies the assumed mode of loading. The reason that the radius of the hole is increased in proportion to L is to maintain strict geometric similarity, which makes it possible to obtain precise information on the size effect, free from the effects of shape (or geometry). The crack profiles are shown in Fig. 1.

The mechanical properties of sea ice vary widely (Sanderson 1988), depending on the type of ice, temperature, and salinity. In the present study, the following typical ice properties are assumed: $f_t' = 0.2$ MPa, $\nu = 0.29$, $E = 1.0$ GPa, and $K_c = 0.1$ MN m$^{-3/2}$ (Sanderson 1988), but some other values are also considered. The specific weight of water, $\rho = 9{,}810$ N/m^3.

The mesh used to calculate the compliance matrices has 60 uniformly spaced angular nodes within one-half of the wedge and 100 nodes on the radial rays. The spacing of the nodes along the radial ray is dense near the hole and is getting gradually coarser farther away [Fig. 2 of part I]. The reason for

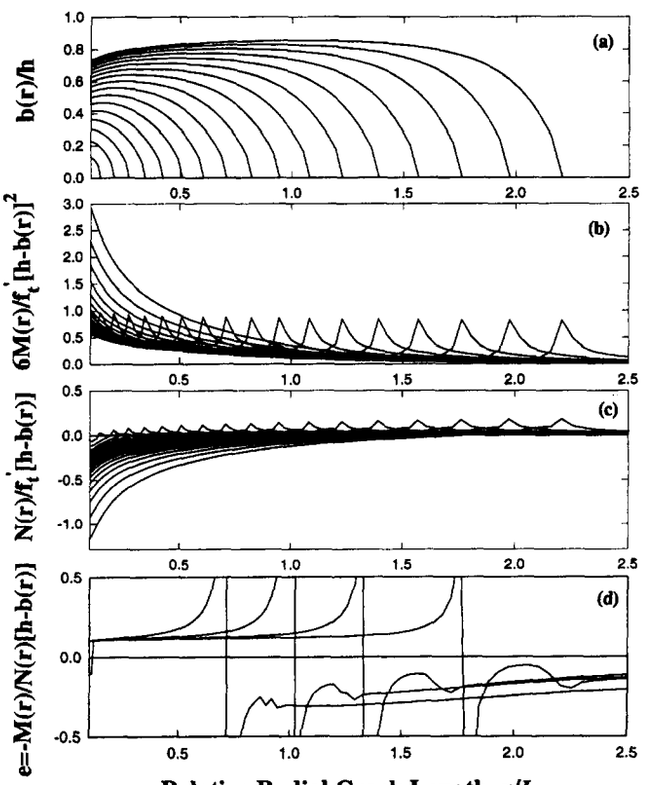

FIG. 1. Calculated Profiles of Nominal Stresses due to Bending Moment and Normal Force, Crack Depth Profiles, and Vertical Shift of Normal Stress Resultant

[1]Walter P. Murphy Prof. of Civ. Engrg. and Mat. Sci., Northwestern Univ., Evanston, IL 60208. E-mail: z-bazant@nwu.edu

[2]Grad. Res. Asst., Dept. of Civ. Engrg., Northwestern Univ., Evanston, IL.

Note. Associate Editor: George V. Voyiadjis. Discussion open until May 1, 1999. Separate discussions should be submitted for the individual papers in this symposium. To extend the closing date one month, a written request must be filed with the ASCE Manager of Journals. The manuscript for this paper was submitted for review and possible publication on March 12, 1998. This paper is part of the *Journal of Engineering Mechanics*, Vol. 124, No. 12, December, 1998. ©ASCE, ISSN 0733-9399/98/0012-1316–1324/$8.00 + $.50 per page. Paper No. 17980.

the variable spacing is twofold: (1) The variation of the compliances near the hole is quite abrupt; and (2) the plastic zone at the crack tip is too short to get resolved with a coarser spacing (but even for the fine spacing used, the plastic zone could not be resolved for thick plates).

Fig. 2(a) shows a few typical load-deflection diagrams plotted as $(\sigma_N - \sigma_e)$ versus $(u - u_e)$, where u_e, σ_e are the load point deflection and nominal stress at the elastic limit, i.e., just before the cracks start to grow. These diagrams terminate at the maximum load state. The maximum load is calculated under the hypothesis that the initiation of the circumferential cracks immediately causes softening in the load-deflection diagram. This hypothesis is based on the experimental observations of Frankenstein (1963). The calculated curves shown in Fig. 2(a) computationally verify the field test results obtained by Frankenstein (1963). However, even if the maximum load occurred only after some finite growth of the circumferential cracks, this hypothesis would be on the safe side.

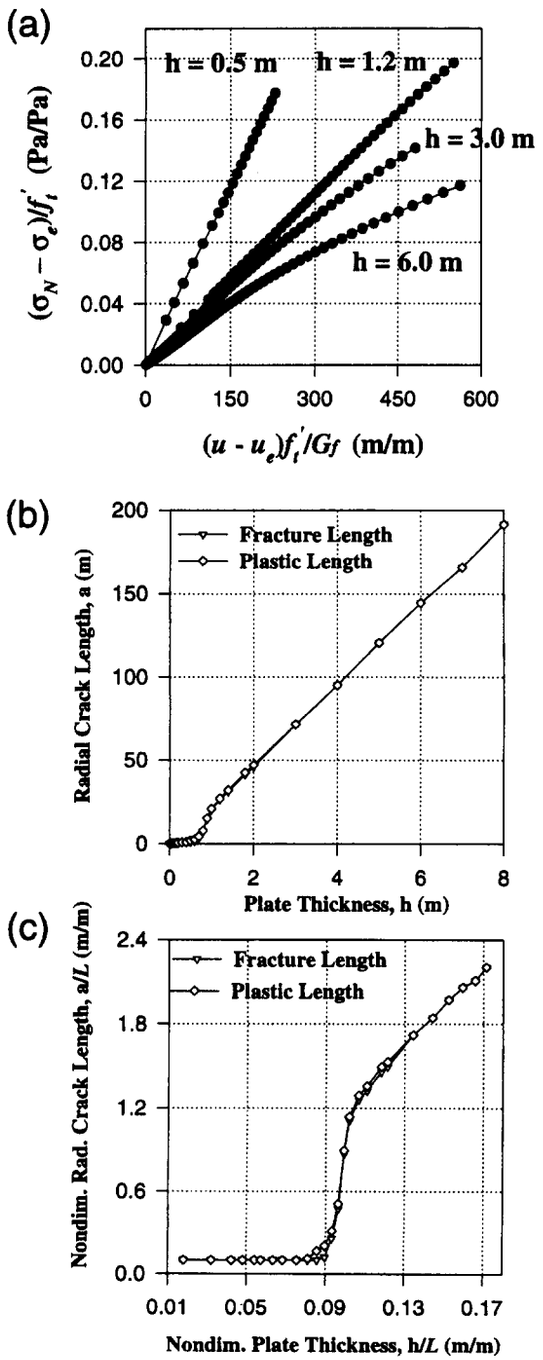

FIG. 2. Plot of: (a) Load-Displacement Diagrams for Plates of Various Thicknesses; (b) Calculated Radial Crack Length As Function of Plate Thickness; (c) Calculated Dimensionless Radial Crack Length As Function of Dimensionless Plate Thickness

Fig. 1 shows the distributions of stress σ_M due to bending moment, stress σ_N due to normal force, and crack depth $b(r)$ along the ray with the crack, calculated for various crack lengths a. The distributions for different loading phases differ. Initially, as the radial crack extends, σ_M and σ_N gradually increase from the first node to the end of the radial crack. Note that, behind the crack front, the bending moment is positive and the normal force is negative. The normal force at the tip of the radial crack is negligible. The crack depth gradually increases as the crack length increases, and the crack edge has a descending slope except near the hole when the crack gets long. As the radial crack becomes sufficiently long, the bending moment profile changes its shape from a gradually ascending profile to a valley-shaped profile with a high peak at the front. The peak would doubtless become a singularity if the plastic zone were negligible and if the nodal spacing approached zero. [Such singularities in the compliance function of a floating plate with many cracks were identified analytically by Dempsey et al. (1995a,b).] The normal force continuously increases behind the crack front. The contribution of the dome effect caused by partial opening of the crack can be judged by comparing the load-deflection diagrams.

When $\alpha \approx 0.4L$, σ_M at the first node is about $0.75L$ and σ_N is about $0.2L$. At that moment, as revealed by Fig. 1, the rate of the vertical crack growth with the radial crack length a slows down near the hole, but no crack unloading [stage 4, Fig. 2(d)] nor shortening (stage 5) ever occurs. The slowing of the vertical crack growth is caused by the development of significant compressive normal forces in the uncracked portion of the ice plate thickness. As the radial crack length reaches about $2.0L$, the vertical crack depth near the hole almost halts its growth and does not exceed the depth beyond about $0.8h$ as the radial crack length increases. The circumferential crack initiates from the radial crack when this limiting vertical crack depth is closely approached.

In the cracked ice plate, a part of the applied load is carried by in-plane normal forces, creating a sort of dome effect. The dome effect is characterized by the distance of the normal force resultant above the middle plane of the plate, which is $\delta(r) = -M(r)/N(r)$. Fig. 1 shows the profiles of $\delta(r)$ at various stages of loading. From these profiles we see that the surface of $\delta(r)$ does not have the simple shape of a dome, but is quite complicated, with positive and negative peaks near the radial crack front. The surface $\delta(r)$ is above the middle plane in the central portion of the plane where the normal compressive forces are high and greatly contribute to the load-carrying capacity. In the outer region, the surface is below the middle plane, but does not cause a significant reduction of load capacity of the plate because in that region the normal forces and bending moments are very small.

SIZE EFFECT AND INFLUENCING PARAMETERS

The size effect is understood as the size dependence of the nominal strength $\sigma_N = P_{max}/h^2$ when geometrically similar structures are compared (P_{max} = maximum load). Characterization of the size effect is the most important benefit of using fracture mechanics. Failures governed by criteria expressed solely in terms of stresses or strains exhibit no size effect (Bažant 1993; Bažant and Chen 1997; Bažant and Planas 1997); i.e., the nominal strength is independent of the structure size when geometrically similar situations are compared. Failures governed by energy criteria and described by fracture me-

chanics generally exhibit a strong size effect (Bažant and Chen 1997; Bažant and Planas 1998), provided that a macroscopically large crack develops prior to the maximum load, as is the case here. Stable formation of such a large crack before failure is typical for quasi brittle materials, that is, materials with a large fracture process zone at the front of a major crack. In view of the in-situ tests reported by Dempsey et al. (1995a,b), Mulmule et al. (1995), and Dempsey (1996), the sea ice on the scale of interest for the penetration problem must be considered to be a quasibrittle material.

The solution may be regarded as a functional relation among eight variables: σ_N, h, G_f, f_t', E, ρ, ν, and a_0. However, as already mentioned, the ratio a/a_0, where a = crack length at breakthrough load P_{max}, may be assumed to be so large that the effect of the radius a_0 of the hole on P_{max} or σ_N is negligible. Furthermore, E, ρ, and ν influence only the elastic deformations of the plate-water system, which are fully characterized by a single parameter, the flexural wavelength L. Therefore, the solution must be given by some function Π of only five variables, $\Pi(\sigma_N, h, G_f, f_t', L) = 0$.

Buckingham's Π-theorem of dimensional analysis (Barenblatt 1979) states that the solution must be reducible to a function of N_v independent dimensionless variables, where $N_v = N_{all} - N_{ind}$; N_{all} = number of all independent variables; and N_{ind} = number of variables with independent physical dimensions. Here we have $N_{all} = 5$ and $N_{ind} = 2$, with the independent physical dimensions being the length and the force. So $N_v = 5 - 2 = 3$. We may choose these variables as indicated in the following form of solution:

$$\frac{\sigma_N}{f_t'} = \Phi\left(\frac{h}{l_0}, \frac{l_1}{l_0}\right) \tag{1}$$

where Φ = some function; $l_0 = EG_f/f_t'^2 = K_c^2/f_t'^2$; and $l_1 = E/\rho \propto L^4/h^3$. Here $K_c = \sqrt{EG_f}$ = fracture toughness (critical stress intensity factor); l_0 = Irwin's (1958) characteristic size of the fracture process zone [introduced for concrete by Hillerborg et al. (1976)]; and l_1 = second independent length parameter. Note that the flexural wavelength $L = [l_1 h^3/12(1 - \nu^2)]^{1/4}$.

The foregoing analysis shows that the elastic properties and specific weight of water influence the solution only through the ratio l_1/l_0. As for the fracture characteristics of ice, G_f and f_t', they influence the solution only through the value of l_0, but not individually. This means that the size effect curve of σ_N/f_t' versus h/l_0 has only one parameter, namely, l_1/l_0.

A set of size effect curves for various values of l_1/l_0 will, therefore, characterize all the possible situations. This conclusion is very useful because the values of G_f as well as f_t' for sea ice exhibit tremendous statistical variability and depend strongly on temperature, salinity, and the size and spacing of voids and channels filled with brine. On the other hand, the value of ρ is a constant and the value of Young's modulus E of ice does not exhibit such a large statistical variability as G_f and f_t'.

The values of Young's modulus E measured by ultrasound range approximately from 4 GPa (5.8×10^5 psi) to 11 GPa (1.6×10^6 psi). Because of the rate effect (or creep), however, the effective E value for static loading is much smaller. In the present computations, the value of E = 1 GPa (1.45×10^5 psi), the same as considered by Evans (1971), was considered as the basic value.

According to the review by Sanderson (1988) and the data of Dempsey et al. (1995a,b), a representative value for the tensile strength f_t' of sea ice is 0.5 MPa (72.5 psi). The value of tensile strength, however, has only a minor effect because the plastic zone at the crack tip is, at maximum load, very small. The fracture toughness K_c is much more important.

Sanderson (1988, page 91), based on small-scale tests, reports K_c-values ranging from 0.044 MPa $m^{-3/2}$ to 0.115 MN $m^{-3/2}$. According to these data and the information from Urabe and Yoshitake (1981) and Weeks and Mellor (1984), the value K_c = 0.1 MN $m^{-3/2}$ [the same as considered by Bažant (1992a,b)] was used in computations. With E = 1 GPa, the corresponding value of fracture energy is G_f = 10 N/m, which was used by Bažant (1992a,b). [For comparison, the thermodynamic surface Gibbs free energy of pure ice is about 0.1 N/m; Ketchum and Hobbs (1969)]. According to Dempsey (personal communication, 1997), the representative value of the fracture energy of sea ice is G_f = 10–15 N/m.

A higher value of fracture energy is indicated by the size effect observed in the large-scale in-situ fracture tests of sea ice recently conducted on the Arctic Ocean near Resolute by Dempsey et al. (1995a,b). The reader is also referred to Mulmule et al. (1995). These tests involved floating notched square specimens of ice 1.8 m thick, with sides ranging from D = 0.5 m to D = 80 m, loaded horizontally by a flat jack inserted into the notch of length $0.3D$ at a distance $0.02D$ from the mouth. The size effect plot of the reported data closely approaches the linear elastic fracture mechanics (LEFM) asymptote of $-1/2$. Dempsey et al. (1995a,b) did not report the fracture energy, but its value can be easily figured out from the maximum load data they reported. To this end, one needs to fit the size effect law to their data, determine the location of the asymptote [as proposed by Bažant and Pfeiffer (1987) and explained in detail in Bažant and Planas (1997)], and use the formula for the stress intensity factor (Tada et al. 1985) for the type of specimen used in these large-scale in-situ tests. The calculation provides K_c = 2.1 MN $m^{-3/2}$ and, for $E \approx 8.8$ GPa, G_f = 520 N/m. With $f_t' \approx 2$ MPa, the characteristic size is then $l_0 \approx 0.5$ m, and $l_1/l_0 \approx 1.8 \times 10^6$. These are the effective values for the whole thickness of ice whose temperature varies from about -20°C on top to about -1°C in contact with seawater.

The values of fracture energy of sea ice depend on its temperature and on the loading rate. They are also different for cracks that grow in the floating ice plate vertically (parallel to grains or columnar crystals, which is called the VH orientation) or horizontally (normal to the grains, which is called the HH orientation) (Mulmule and Dempsey 1997).

The values from Dempsey et al.'s tests near Resolute, however, are pertinent to horizontal propagation of a long full-through vertical crack. In our problem, the crack propagates mainly vertically, which doubtless causes the fracture process zone to be smaller than in Dempsey's tests, and thus the effective fracture energy to be lower. Also, the anisotropy of sea ice is likely to cause the effective fracture energy for vertical crack propagation to be less than that for horizontal propagation, because the fracture runs along, rather than across, the vertical hexagonal columnar crystals of sea ice and along, rather than across, the vertical brine channels. This gives another reason why the fracture energy for the penetration problem should be considered smaller than in Dempsey et al.'s tests near Resolute.

In view of the preceding discussion, the representative value of the characteristic size of the fracture process zone for the present computations is chosen as l_0 = 0.25 m, with the ratio $l_1/l_0 = 4.5 \times 10^5$. The size effect results for these parameters and for the failure mode with six cracks in a star pattern are shown by the data circles in the bilogarithmic plot in Fig. 3(a).

To obtain information on the effect of parameter l_1/l_0, additional computations have been run for the value $l_1/l_0 = 3.9 \times 10^4$. These are shown by the data squares in Fig. 3(a). It is immediately apparent from this figure that the difference between the trends of the data circles and data squares is rather small. This is not surprising, since l_1 and l_0 differ by several orders of magnitude, which means that they can hardly interact. Therefore, the effect of parameter l_1/l_0 can be neglected.

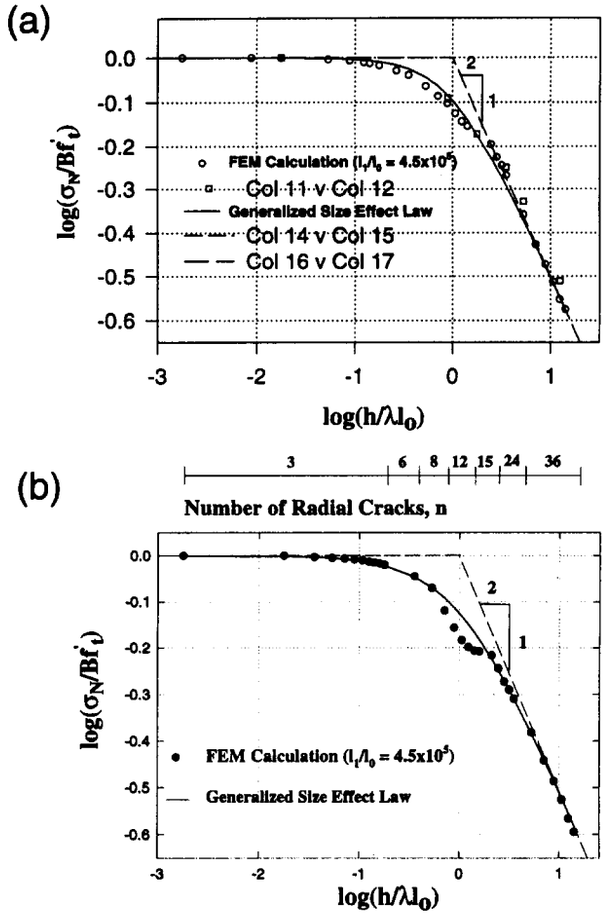

FIG. 3. Diagram of: (a) Size Effect Calculated for Fixed Number of Radial Cracks, $n = 6$; (b) Size Effect Calculated for Thickness Dependent Number of Radial Cracks Determined from Crack Initiation Analysis

(Values of $l_1/l_0 \geq 10^6$ have caused convergence problems, apparently because the fracture process zone in that case is too small to be resolved for large ice thicknesses by the assumed mesh.)

The calculated data circles in Fig. 3(a) trace a relatively smooth curve, except for a steep bump in the middle. This bump appears associated with the rapid rise in ratio a/h seen in Fig. 2(b,c), which occurs when h increases from 0.5 m to 1 m. For small thicknesses, approximately $h \leq 20$ cm, the radial crack length at maximum load remains approximately constant, which may be explained by the fact that the fracture process zone (or l_0) is not small compared to the plate thickness. In that case, the strength theory must be expected to apply, and indeed the size effect curve is initially horizontal. For thick plates, approximately for $h \geq 1$ m, the radial crack length at maximum load in Fig. 2(b,c) is approximately proportional to the flexural wavelength L (or to $h^{3/4}$). In that case, the quasibrittle size effect law should be followed, and it indeed is. If a/L did not approach a constant for thick enough plates, the size effect plot would not approach an asymptote of slope $-1/2$.

DEPENDENCE OF SIZE EFFECT ON NUMBER OF CRACKS

The dependence of the number of cracks on the plate thickness was studied in a second round of computations. For this purpose, one needs first to understand crack initiation from the smooth surface of the hole on which the vertical distributed load is assumed to be applied.

A simple method for determining the spacing of cracks initiating from the smooth surface of a half-space was proposed by Bažant et al. (1979) [see also Bažant and Cedolin (1991, section 12.6)] and was recently refined by Li and Bažant (1994) and Li et al. (1995). The method involves three conditions: (1) The stress before crack initiation attains the material tensile strength; (2) the energy release caused by the formation of cracks of finite initial length a_i is equal to the surface energy of these cracks determined from the fracture energy G_f of the material; and (3) the cracks of initial length a_i are in a critical state; i.e., their energy release rate is equal to G_f. These three conditions have also been applied by Li et al. (1995) to the crack spacing in highway pavements. The last two conditions imply the neglect of possible acoustic radiation of energy, and possible additional energy dissipation by distributed damage that is not included in G_f.

From the foregoing three conditions, one can determine the load level at which the initial cracks form, their initial length a_i, and their spacing. Li and Bažant (1994) deduced from these three conditions the number n_c of radial cracks initiating from a hole in the ice plate, as indicated in Table 1 of the companion paper; n_c increases from three cracks for ice plates under $0.1L$ thick, to 36 cracks for ice plates over $5L$ thick.

Taking the numbers of radial cracks for various ice thicknesses from the analysis of Li and Bažant (1994), and running the present computer program for each of these numbers, we obtain the size effect plot shown in Fig. 3(b). The numbers of radial cracks for various size ranges are indicated in the figure.

Comparing this figure with the previous Fig. 3(a) for $n_c = 6$, we see that the effect of the number of cracks is not strong (which is a similar conclusion to that of the plastic limit analysis of the penetration problem). The overall curvature of the size effect plot is only slightly less than in the previous case. The horizontal small-size asymptotic slope is slightly higher for the varying wedge angle analysis than for the constant angle analysis. The average slope between 0.001 m and 0.05 m plate thickness is 6.084×10^{-3} and 7.744×10^{-3} for Figs. 3(a) and 3(b), respectively, and the percent difference between the slopes is 0.21%. The large-size inclined asymptote, which has again the slope of $-1/2$, is slightly lower for the varying angle case than for the constant angle case. The slopes are 0.502 and 0.463 for Figs. 3(a) and 3(b), respectively, and the percent difference is 0.08%. The numerical results for varying numbers of cracks can again be closely described by Bažant's generalized size effect law in (2), in which $\lambda_0 = 2.55$, $m = 1/2$, $r = 1.2$, and $l_0 = 0.25$ m. This law is shown in Fig. 3(b) by the continuous curve.

ANALYSIS OF SIZE EFFECT RESULTS

The size effect was initially studied under the assumption of full-through bending cracks for which the large size behavior was found to be $\sigma_N \propto h^{-3/8}$, as confirmed by the studies of Slepyan (1990), Bažant (1992a,b), Bažant and Li (1994a,b), and Li and Bažant (1994). [For long full-through thermal bending cracks, a similar size effect was found by Bažant (1992a,b).] The reason why for full-through cracks the asymptotic size effect is not $\sigma_N \propto h^{-1/2}$ is because the plate thickness h is actually not a dimension in the plane (x, y) of the boundary value problem of the infinite floating plate, but merely a parameter giving the cylindrical stiffness D. No physical dimension in the plane (x, y) exists (except for the hole, whose effect is, however, considered negligible). The only dimension present is the flexural wavelength L, which depends on the thickness as $L \propto h^{3/4}$. Thus, for full-through fracture, the size effect must be expected in the form $\sigma_N \propto L^{-1/2}$, or $\sigma_N \propto (h^{3/4})^{-1/2} \propto h^{-3/8}$. This was evidenced by the penetration studies of Slepyan (1990), Bažant (1992a,b), Bažant and Li (1994a,b), and Li and Bažant (1994) [and for thermal fracture, Bažant (1992a,b)].

A different asymptotic size effect, however, is exhibited by the present numerical solution. As seen in Figs. 3(a) and 3(b), the large-size asymptote of the size effect curve has the slope $-1/2$, i.e., $\sigma_N \propto h^{-1/2}$ for $h \to \infty$, which is the standard asymptotic size effect. The reason why the asymptotic size effect $\sigma_N \propto h^{-3/8}$ does not apply is because the crack is not full-through, but is growing across the plate thickness, which is a standard crack propagation problem. Even though the numerical solution is two-dimensional (in the horizontal plane), the fracture propagates only in the third dimension and its behavior is embedded in the Rice-Levy springs. An interesting theoretical question is whether the (3/8)-power law for full-through cracks can be obtained as a limiting case of the present solution. The answer is no, because the Rice-Levy springs cannot simulate the conditions at the tip of a horizontally propagating full-through bending crack.

In a recent simplified solution of Dempsey et al. (1995a,b), in which the depth of part-through cracks was assumed to be constant over the entire crack length, the ice was assumed to follow LEFM, and the case of many cracks was considered, the size effect was of the type $\sigma_N \propto h^{-1/2}$ for all h.

As is typical of quasi brittle fracture (Bažant 1984; Bažant and Chen 1997; Bažant and Planas 1998), the small-size asymptote of the calculated size effect plot in Fig. 3(a) is horizontal and corresponds to a solution according to plastic limit analysis (strength theory), whose applications to the penetration problem were reviewed by Kerr (1996) [see also Sodhi (1995a,b, 1996)]. The present computations show that plastic limit analysis (strength theory) corresponding to the horizontal asymptote of the size effect plot, is a good enough approximation only for ice thicknesses up to about 0.2 m (assuming that $l_0 = 0.25$ m). At the same time, the σ_N values for the horizontal asymptote can scatter widely, depending on the type of ice and the environmental conditions (air and water temperature). This may explain why no size effect was observed in small-scale laboratory experiments.

The large-size asymptote of the size effect plot, which has the slope of $-1/2$ corresponding to LEFM, is seen to be a good enough approximation for ice thicknesses over 1.0 m. The value of parameter λ_0 is chosen so that $h = \lambda_0 l_0$ would represent the thickness at the intersection point of the two asymptotes. From the present numerical results, $\lambda_0 = 2.26$. The ratio $\beta = h/(\lambda_0 l_0)$ determined in this manner has been called the brittleness number (Bažant 1987; Bažant and Pfeiffer 1987; Bažant and Planas 1997). The limit $\beta \to \infty$ indicates the perfectly brittle response, i.e., LEFM, and the limit $\beta \to 0$ indicates the perfectly ductile (plastic) response.

The present numerical results, spanning over four orders of magnitude of ice thickness, can be closely fitted by the generalized form of Bažant's size effect law (Bažant 1985; Bažant and Pfeiffer 1987; Bažant and Chen 1997; Bažant and Planas 1998), shown by the continuous curve in Fig. 3(a)

$$\frac{\sigma_N}{Bf_t'} = \left[1 + \left(\frac{h}{\lambda_0 l_0}\right)^r\right]^{-1/2r} \tag{2}$$

Here, the dimensionless parameters found by fitting of the numerical results are $B = 1.214$; $\lambda_0 = 2.55$; $m = 1/2$; $r = 1.55$; the dimensional parameters used in Fig. 3 are $l_0 = 0.25$ m; and $f_t' = 0.2$ MPa (from which $K_c = f_t'\sqrt{l_0} = 0.1$ MN m$^{-3/2}$). This approximate law has been derived as the asymptotic matching between the large-size and small-size expansions of the size effect (Bažant 1995a,b, 1997).

Eq. (1) can be written as $Y = AX + C$, where $X = h^r$, $Y = (\sigma_N)^{-2r}$, $A = (Bf_t')^{-2r}$, and $C = 1/(\lambda_0 l_0 Bf_t'^2)^r$. This means that, if r is known, the values of Bf_t' and $\lambda_0 l_0$ can be determined by linear regression. The regression may be conducted for various chosen r values such that the optimum r is found.

With the aforementioned dimensionless values of B, λ, m, and r, (2) can be used as a general approximate prediction formula, provided, of course, the values of l_0 and f_t' are known.

The present numerical results confirm that the (3/8)-power law previously obtained for full-through cracks is not applicable. The (3/8)-power law would apply when the horizontal forces are sufficiently small compared to the bending moments. This would have to happen for a floating plate that is sufficiently thin and sufficiently fragile so as to fail by fracture rather than by plastic yielding. Such conditions may be expected to occur when $l_0 \ll h \ll L$. But this does not occur in the realistic range of ice properties.

The (3/8)-power law does, nevertheless, apply to the scaling of the critical temperature difference that can produce long thermal fractures running in a stationary state, analyzed by Bažant (1992a,b). The reason is that, despite the presence of a large fracture process zone with a part-through crack, there exists around the front of a long enough crack a control region that moves with the crack front, remains in a stationary state, and is so large that ahead of this region there is no deflection and no damage, while behind this region there is a full-through crack if the crack is long.

Another interesting plot is that of the radial crack length a versus ice thickness h, shown in Fig. 2(b). Two values of a are shown: the length to the front of the plastic zone at the bottom surface of the plate, and the length to the front of the open LEFM crack. As can be seen, both crack lengths are very close and are undistinguishable for large thicknesses. This means that the plastic behavior is not important for the overall response, and confirms that a very accurate but complex modeling of the plastic zone at the crack front is not necessary. The reason that no plastic crack length is seen in Fig. 2(b) for large plate thicknesses is that the nodal spacing is increased in proportion to the ice thickness. For thick plates the nodal spacing becomes larger than the length of the plastic zone. This is clear from Fig. 2(c), showing the dimensionless crack length a/L versus dimensionless ice thickness h/L.

COMPARISONS WITH TEST DATA

The present results on the number of cracks roughly agree with the field observations of Frankenstein (1963, 1966) and Lichtenberger et al. (1974). Frankenstein made extensive observations on lake ice, which can be assumed to behave similarly as sea ice. Despite irregularities in the observed crack patterns, Frankenstein's tests clearly show that the number n_c of cracks increases with the ice thickness h.

The aforementioned experimental data on the size effect in penetration of sea ice were analyzed by Sodhi (1995a,b, 1996) under the assumption that sea ice is a plastic material. Sodhi concluded that these data confirm the absence of size effect, which is characteristic of his solution based on plasticity.

However, this conclusion is due solely to a questionable statistical treatment of the data. Sodhi (1995a) based his conclusion on the plot of P_{max} versus h, as shown in Fig. 4(a). This kind of plot seems, indeed, to suggest that P_{max} is approximately proportional to h^2, which would mean that σ_N is constant, free of size effect. However, such a way of reasoning is deceptive. The main reason is that, implicitly, a strong deterministic variation obscuring the size effect, namely, the proportionality of P_{max} to h^2, has been superposed on the test data by Sodhi's choice of coordinates of the plot.

What a misleading effect such a choice of coordinates can have is illustrated in Figs. 4(b and c). In Fig. 4(b), we assume hypothetical perfect data, conforming exactly to Bažant's size effect law. Then we plot the same data in the graph of log P_{max} versus log h [Fig. 4(c)]. According to Sodhi's viewpoint that there is no size effect, one would pass the regression line of slope 2 shown in the figure. The comparison of this regression line with the data seems now acceptable, indicating

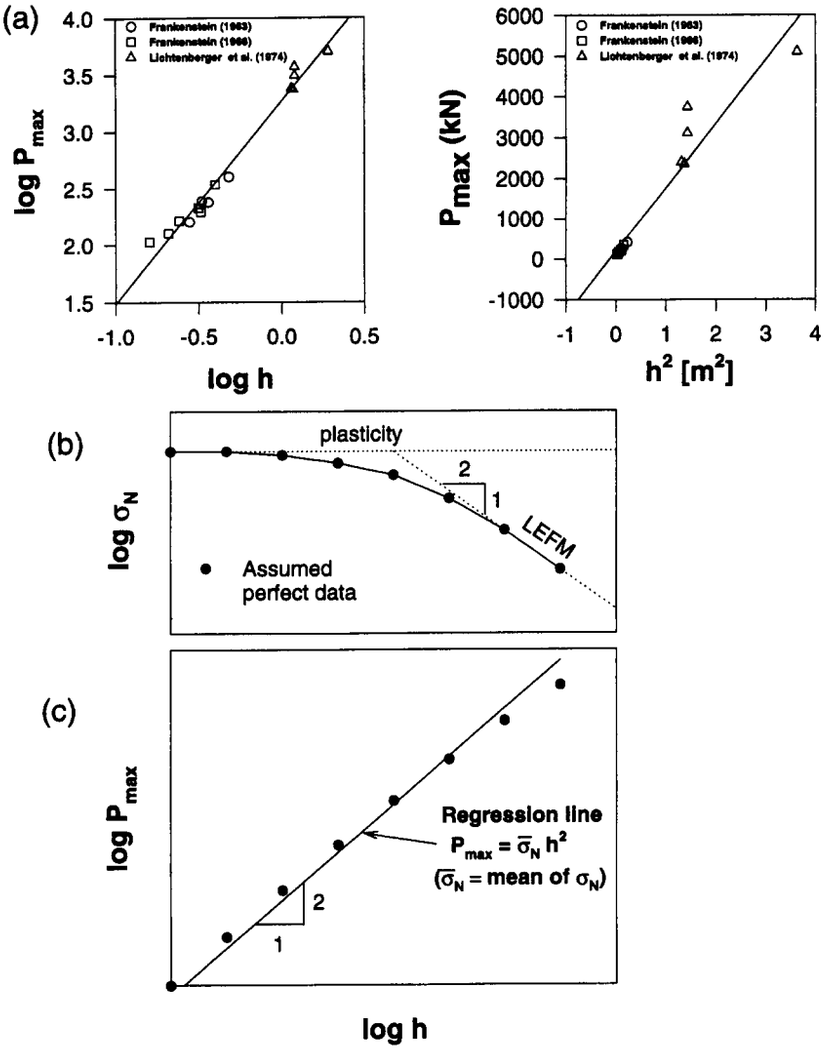

FIG. 4. Diagram of: (a) Sodhi's Way of Plotting Existing Test Data; (b) Incorrect Choice of Coordinates for Statistical Analysis; (c) Incorrect Choice of Coordinates for Statistical Analysis

a relatively low coefficient of variation of the deviations from the regression line. The comparison would look even more acceptable if the inevitable random scatter were superposed. Yet this is the case of perfect agreement with the size effect law.

A second questionable aspect of Sodhi's (1995a,b) evaluation of test data is that he correlated in the same diagram the test results from different test series while implying the same ice properties. However, the ice properties were most likely quite different. If the differences in ice properties among the two test series of Frankenstein (1963, 1966) and that of Lichtenberger et al. (1974) were taken into account, the groups of data points for these tests could shift vertically in the plot in Fig. 4(a). Thus, what looks like a good agreement with the proportionality of P_{max} to h^2 could be lost by such vertical shifts. It is probably by chance that the differences among the ice properties compensated for the size effect.

Since the size effect is the deviation from the proportionality of P to h^2, the only nonobfuscating way that can bring the size effect to light is to plot the values of $\sigma_N = P/h^2$; i.e., to construct the plot of the measured values of $\log \sigma_N = \log(P/h^2)$ versus $\log h$ (rather than a plot of P versus h). Because the ice properties in different test series were not the same, the plots intended to check for size effect should be made separately for each test series. This is done in Fig. 5(a) for the three data series reported by Frankenstein (1963, 1966) and Lichtenberger et al. (1974). Looking at these plots now leads to a conclusion very different from Sodhi's: There is a clear size effect in each test series.

Furthermore, Fig. 5(b) shows the linear regression plots of $1/\sigma_N^2$ versus h, in which the size effect law (2) with $r = 1$ is represented by the regression line. These linear regression plots make it possible to determine the coefficients of variation of the slope of the regression line. However, the data are too few and the size range too narrow to obtain meaningful statistics.

Finally, Fig. 5(c) shows all three data sets in one plot of $\log(\sigma_N/Bf_t')$ versus $\log(h/\lambda_0 l_0)$, and in another plot of $(Bf_t'/\sigma_N)^2$ versus $h/\lambda_0 l_0$. These unified plots use the optimum values of Bf_t' and $\lambda_0 l_0$ obtained by a previous separate regression of each data set. These two plots [Fig. 5(c)] confirm that the present theory is in overall acceptable agreement with the available test results.

In view of the high scatter and limited size range of the available data, it cannot be claimed, however, that the existing test results actually prove the present theory. There might exist another theory that fits these limited data also. The answer to this question and the verification for large ice thicknesses will have to await measurements of a much broader size range. Nevertheless, all the plots in Fig. 5 visually demonstrate the invalidity of Sodhi's claim that there is no size effect.

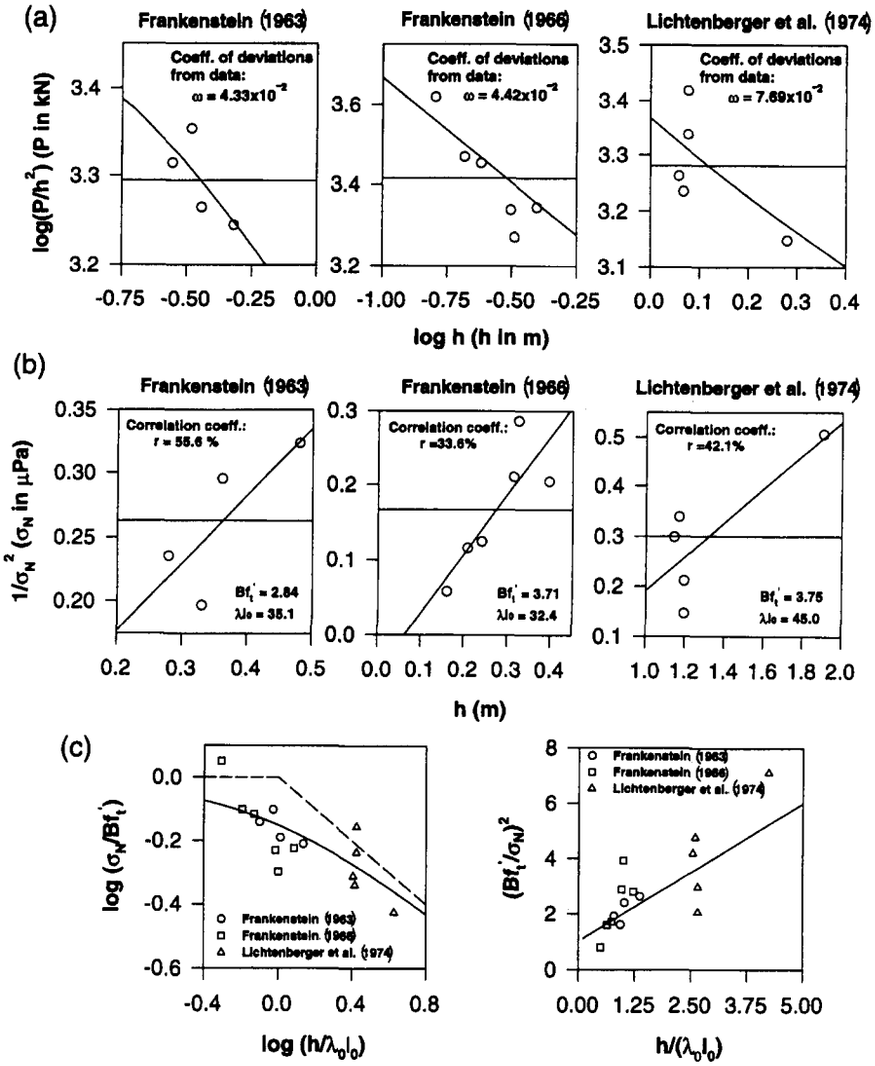

FIG. 5. Comparison of Present Theory with Test Data from Literature

SOME REMAINING QUESTIONS

Although the present study probably answers the main questions in the ice penetration problem, several questions still remain. Due to temperature variations through the ice plate and diffusion of brine, the ice plate is not homogeneous. Its bottom, where the temperature is near the melting point, is very soft and weak, while the top is cold and thus stiff and strong. The present analysis must be interpreted in the sense of a certain effective ice thickness that gives about the same bending stiffness as that of the actual ice plate, and the values of K_f, f_t', and E must be interpreted as the equivalent effective properties throughout the thickness. An accurate analysis, however, would have to take these differences into account.

Another question is the neglect of the rate of loading. Sea ice exhibits creep, and the effective fracture energy as well as the strength depend on the rate of crack growth. Regarding the number of cracks, there is another phenomenon that may play a role. It could happen that some of the radial cracks could grow longer than others. A bifurcation of the equilibrium path, in which a bifurcated solution with unequal crack lengths may be followed, is a possibility. This problem could be analyzed similarly to the problem of bifurcation and changes of spacing in the evolution of a system of parallel cooling cracks in a half-space (Bažant et al. 1979; Bažant and Cedolin 1991, section 12.6). Analysis of this problem would require abandoning the present assumption of symmetry of response.

Finally, the value of l_0 might be larger for a thicker ice plate, because of its higher heterogeneity.

CONCLUSIONS

1. The mechanism of penetration of a floating sea ice plate involves the growth of radial cracks that cut only through a part of the ice thickness. The crack depth at maximum load is about 80% of the ice thickness.
2. The nominal strength of the sea ice plate exhibits a strong size effect. For small ice thicknesses (up to about 0.2 m), the size effect can be neglected. For large thicknesses (exceeding about 1 m), the logarithmic size effect plot approaches an asymptote of slope $-1/2$, which is typical of LEFM. The previously derived asymptote of slope $-3/8$, which corresponds to full-through cracks, cannot occur for realistic properties of sea ice.
3. The characteristics of an effective numerical model are as follows: (1) The cracked radial section is subdivided into vertical strips in which the crack is assumed to grow upward, independently of the cracks in the adjacent strips; (2) the cracked vertical strip is modeled by the Rice-Levy nonlinear softening line spring; (3) a yield criterion is adopted to decide crack initiation in the vertical strips, and the initial plastic crack growth follows a nonassociated LEFM flow rule; (4) compliance matrices are used to characterize the uncracked sector of the ice

plate on the elastic foundation; (5) the Levenberg-Marquardt nonlinear optimization algorithm is used to solve a large system of nonlinear equations based on the initial estimate provided by the solution of the previous loading step; and (6) the maximum load is calculated under the assumption that the initiation of the circumferential cracks immediately causes softening in the load-deflection diagram.

4. The previously established dependence of the number of radial cracks on the ice thickness does not have a strong influence on the size effect plot.
5. Dimensional analysis shows that, with some mild simplifications, the dimensionless nominal strength of the plate depends on only two parameters—the dimensionless size and the dimensionless elastic modulus of ice. The latter is further shown to have little influence. Consequently, one dimensionless size effect curve can approximate the response in general.
6. The existing field measurements of size effect agree with the present theory well, although their size range is too limited for actually proving the theory. Sodhi's opinion that there is no size effect is invalid for ice plates thicker than about 20 cm.
7. Until calibration by more extensive test data becomes possible, based on (1) it is recommended to predict the static load capacity of the sea ice plate from Fig. 3(b) or, approximately, from the formula

$$P_{max} = \frac{1.214 f_t' h^2}{[1 + (h/2.55l_0)^{1.55}]^{1/3.1}}$$

APPENDIX I. LEVENBERG-MARQUARDT NONLINEAR OPTIMIZATION ALGORITHM

The Levenberg-Marquardt iterative algorithm (Levenberg 1944; Marquardt 1963) combines the best features of the inverse-Hessian method and the steepest descent method to minimize the sum of squares of m nonlinear functions f_i on n-dimensional vector $\mathbf{x}$ (column matrix); $\mathbf{f}^2(\mathbf{x}) = \sum_{i=1}^{m} f_i^2(\mathbf{x}) = \min$. In the initial iterations, when the trial values are not close to the solution, the steepest descent method (or gradient method) is used

$$\mathbf{x}_{next} = \mathbf{x}_{trial} - \text{const.} \times \nabla \mathbf{f}^2(\mathbf{x}) \tag{3}$$

where $\mathbf{f}$ = column matrix of components f_i, and the constant must be chosen small enough. In proximity of the correct solution, the inverse-Hessian method is used to converge rapidly to the best estimate

$$\mathbf{x}_{best} = \mathbf{x}_{trial} + \mathbf{H}^{-1}[-\nabla \mathbf{f}^2(\mathbf{x})] \tag{4}$$

where $\mathbf{H}$ = Hessian matrix whose components are the second partial derivatives of the function. To judge the accuracy, the algorithm also calculates the standard deviations of the initial guess of the solution and of the final solution.

ACKNOWLEDGMENTS

Financial support under grant N00014-91-J-1109 (monitored by Dr. Y. Rajapakse) from the Office of Naval Research to Northwestern University is gratefully acknowledged.

APPENDIX II. REFERENCES

Barenblatt, G. I. (1979). *Similarity, self-similarity and intermediate asymptotics*. Consultants Bureau, New York.

Bažant, Z. P. (1984). "Size effect in blunt fracture: Concrete, rock, and metal." *J. Engrg. Mech.*, ASCE, 110, 518–535.

Bažant, Z. P. (1985). "Fracture mechanics and strain-softening in concrete." *U.S.-Japan Seminar on Finite Element Anal. of Reinforced Concrete Struct.*, Preprints, 1, 47–69.

Bažant, Z. P. (1992a). "Large-scale fracture of sea ice plates." *Proc., 11th IAHR Ice Symp.*, T. M. Hrudey, ed., IAHR, Delft, The Netherlands, 2, 991–1005 (held in Banff, Canada).

Bažant, Z. P. (1992b). "Large-scale thermal bending fracture of sea ice plate." *J. Geophys. Res.—Oc.*, 97(C11), 17739–17751.

Bažant, Z. P. (1993). "Scaling laws in mechanics of failure." *J. Engrg. Mech.*, 119(9), 1828–1844.

Bažant, Z. P. (1995a). "Scaling of quasibrittle fracture and the fractal question." *J. Mat. and Technol.*, 117(Oct.), 361–367.

Bažant, Z. P. (1995b). "Scaling theories for quasibrittle fracture: Recent advances and new directions." *Fracture mechanics of concrete structures. Proc., 2nd Int. Conf. on Fracture Mech. of Concrete and Concrete Struct. FraMCoS-2*, F. H. Wittmann, ed., Aedificatio Publishers, Freiburg, Germany, 515–534 (held at ETH, Zürich).

Bažant, Z. P. (1997). "Scaling of quasibrittle fracture: Asymptotic analysis." *Int. J. Fracture*, 83(1), 19–40.

Bažant, Z. P., and Cedolin, L. (1991). *Stability of structures: Elastic, inelastic, fracture and damage theories*. Oxford University Press, New York.

Bažant, Z. P., and Chen, E.-P. (1997). "Scaling of structural failure." *Appl. Mech. Rev.*, 50(10), 593–627.

Bažant, Z. P., and Kim, J. J. H. (1998). "Size effect in penetration of sea ice plate with part-through cracks. I: Theory." *J. Engrg. Mech.*, ASCE, 124(12), 1310–1315.

Bažant, Z. P., and Li, Y.-N. (1994a). "Penetration fracture of sea ice plate: Simplified analysis and size effect." *J. Engrg. Mech.*, ASCE, 120(6), 1304–1321.

Bažant, Z. P., and Li, Y.-N. (1994b). "Penetration through floating sea ice plate and size effect: Simplified fracture analysis." *J. Engrg. Mech.*, ASCE, 120(7), 1304–1321.

Bažant, Z. P., Ohtsubo, R., and Aoh, K. (1979). "Stability and post-critical growth of a system of cooling and shrinkage cracks." *Int. J. Fracture*, 15, 443–456.

Bažant, Z. P., and Pfeiffer, P. A. (1987). "Determination of fracture energy from size effect and brittleness number." *ACI Mat. J.*, 84, 463–480.

Bažant, Z. P., and Planas, J. (1998). *Fracture and size effect in concrete and other quasibrittle materials*. CRC Press, Boca Raton, Fla.

Dempsey, J. P. (1996). "Scale effects on the fracture of ice." *The Johannes Weertmann Symp.*, R. J. Arsenault et al., eds., The Minerals, Metals and Mat. Soc. (TMS), Warrendale, Pa., 351–361.

Dempsey, J. P., Adamson, R. M., and Mulmule, S. V. (1995a). "Large-scale in-situ fracture of ice." *Proc. FraMCoS-2*, F. H. Wittmann, ed., Aedificatio Publishers, D-79104, Freiburg, Germany (held in Zürich).

Dempsey, J. P., Slepyan, L. I., and Shekhtman, I. I. (1995b). "Radial cracking with closure." *Int. J. Fracture*, 73(3), 233–261.

Frankenstein, E. G. (1963). "Load test data for lake ice sheet." *Tech. Rep. 89*, U.S. Army Cold Regions Res. and Engrg. Lab., Hanover, N.H.

Frankenstein, E. G. (1966). "Strength of ice sheets." *Proc., Conf. on Ice Pressures against Struct., Tech. Memorandum No. 92, NRCC No. 9851*, Laval Univ., Québec, PQ, Nat. Res. Council of Canada, 79–87.

Hillerborg, A., Modéer, M., and Petersson, P. E. (1976). "Analysis of crack formation and crack growth in concrete by means of fracture mechanics and finite elements." *Cement and Concrete Res.*, 6, 773–782.

Kerr, A. D. (1996). "Bearing capacity of floating ice covers subjected to static, moving, and oscillatory loads." *Appl. Mech. Rev.*, 49(11), 463–476.

Levenberg, K. (1944). "A method for the solution of certain nonlinear problems in least-squares." *Quarterly Appl. Mathematics*, 2, 164–168.

Li, Y.-N., and Bažant, Z. P. (1994). "Penetration fracture of sea ice plate: 2D analysis and size effect." *J. Engrg. Mech.*, ASCE, 120(7), 1481–1498.

Li, Y.-N., Hong, A. N., and Bažant, Z. P. (1995). "Initiation of parallel cracks from surface of elastic half-plane." *Int. J. Fracture*, 69, 357–369.

Lichtenberger, G. J., Jones, J. W., Stegall, R. D., and Zadow, D. W. (1974). "Static ice loading tests, Resolute Bay—Winter 1973/74." *APOA Proj. No. 64, Rep. 745B-74-14 (CREEL Bib. No. 34-3095)*, Sunoco Sci. and Technol., Richardson, Tex.

Marquardt, D. W. (1963). "An algorithm for least-squares estimation of nonlinear parameters." *J. Soc. Industrial Appl. Mathematics*, 11, 431–441.

Mulmule, S. V., and Dempsey, J. P. (1997). "Stress-separation curves for saline ice using fictitious crack model." *J. Engrg. Mech.*, ASCE, 123(8), 870–877.

Mulmule, S. V., Dempsey, J. P., and Adamson, R. M. (1995). "Large-

scale in-situ ice fracture experiments—Part II: Modeling aspects." *Ice mechanics—1995*, J. P. Dempsey and Y. Rajapakse, eds., ASCE AMD, New York, 207, 129–146.
Sanderson, T. J. O. (1988). *Ice mechanics: Risks to offshore structures.* Graham and Trotman Limited, London.
Sodhi, D. S. (1995a). "Breakthrough loads of floating ice sheets." *J. Cold Reg. Engrg.*, ASCE, 9(1), 4–20.
Sodhi, D. S. (1995b). "Wedging action during vertical penetration of floating ice sheets." *Ice mechanics—1995*, J. P. Dempsey and Y. Rajapakse, eds., ASME AMD, New York, 207, 65–80.
Sodhi, D. S. (1996). "Deflection analysis of radially cracked floating ice sheets." *17th Int. Conf. OMAE Proc., Book No. G00954*, 97–101.
Tada, H., Paris, P. C., and Irwin, G. R. (1985). *Stress analysis of cracks handbook.* Del Research Corp., Hellertown, Pa.

SIZE EFFECT IN PENETRATION OF SEA ICE PLATE WITH PART-THROUGH CRACKS. I: THEORY. II: RESULTS[a]

Discussion by J. P. Dempsey[3]

A thorough examination of the quasi-static penetration of a floating elastic-brittle plate via a fracture mechanics approach has been presented by Bažant and Kim. Bažant and Kim reach the conclusion that there is a size effect (in terms of the plate thickness, h). A few of the assumptions made by these authors will be examined in this discussion.

The formulation presented by Bažant and Kim assumes both that a radial system of part-through cracks is formed and that the appearance of these radial cracks is accompanied by stable crack growth. The analysis proceeds by subdividing each part-through crack into narrow vertical strips (the ith strip being of length b_i, with ligament $h - b_i$). In each strip, the crack is assumed to propagate vertically, independently of the crack propagation in the adjacent strips. A simplified form of a cohesive crack model is adopted, with the crack initially growing as a plastic crack.

The assumed stable development of the part-through radial cracks does not match experimental observations, especially for thin to moderately thick ice sheets ($h < 0.5$ m). The initiation of cracks in ice almost always leads to unstable crack growth (DeFranco and Dempsey 1994). The radial cracking that occurs prior to the formation of circumferential cracks and subsequent penetration is understood to occur suddenly and to be through-the-thickness. In other words, a system of through-the-thickness radial cracks occurs, with rapid radial and through-the-thickness crack propagation. Even though these radial cracks are subjected to the dome or arching effect, crack growth instability in ice is sufficient to allow through-the-thickness cracks to form (in thick ice sheets, it is plausible to assume that the through-the-thickness cracking would be prevented by the arching effect). Dempsey et al. (1995) studied radial cracking with closure for the case of a clamped plate subjected to a concentrated lateral load. By assuming that the closure width was a function of the radial crack length only, Dempsey et al. (1995) obtained an analytical solution that facilitated a thorough examination of the dependencies of the closure width, the nucleated radial crack lengths, the energy release rate, and the penetration load. In particular, the latter analysis made it clear that radial crack growth instability would accompany the nucleation of any radial crack system. A finite-element study of a radially cracked floating plate by Sodhi (1996) confirmed the broad applicability of the conclusions reached by Dempsey et al. (1995).

An implicit requirement underlying the size effect analysis presented by Bažant and Kim is the stable formation of process zones (contiguous to each traction-free crack front) that scale self-similarly with the ice sheet thickness. However, if sudden and unstable radial crack formation takes place, with full through-the-thickness crack-face separation and subsequent compressive closure (unilateral contact, in other words), there is no logical way in which one can simultaneously assume the stable formation of process zones; there are, in fact, no ligaments subjected to bending, but instead pairs of completely separated crack faces subjected to ever-increasing pressure due to the arching action. This pressure grows to be of such magnitude that zones of circumferential microcracking in the plane of the ice sheet have been observed to occur, at variable radial distances away from the load. The radial crack lines have been observed to ''whiten'' with intense microcracking (Frankenstein 1966), and this is consistent with unilateral contact conditions of the receding type (Dundurs 1995), in which the extent of contact remains invariable with increasing load (in the case of elastic media; creep may alter this behavior, but not significantly). The issue of crack growth stability and whether the radial cracks would form stably or unstably was bypassed by Bažant and Kim, since they adopted the radial crack length a as the controlled variable. Their formulation, therefore, does not include a condition related to crack growth stability. By controlling the radial crack length numerically, their crack growth simulation is more stable than could be obtained in ice even under closed loop displacement controlled loading. For the majority of situations encountered, the much less stable condition of load control is operative.

For the case of relatively thick ice sheets, it is plausible that a radial crack system could form that would be comprised of part-through cracks. These part-through cracks would still form suddenly and, because of crack growth instability, would immediately partially close, with conditions of $K = 0$ along the crack front. Even on further loading, the remaining ligaments would be subjected to the compression induced by arching, and only during load-up would the crack fronts experience tension and process zone growth. The stable formation of crack-tip contiguous—but not necessarily self-similar—process zones would be expected to occur, but only for the case of rather thick ice sheets (thick here is estimated to mean $h \geq 1$ m).

If there is a size effect in ice thickness, it is important that it be determined, especially from the viewpoint of vehicles landing on, or traveling on, the ice. Safety is of primary concern in this case, and breakthrough is to be avoided. However, for the case of submarine surfacing, successful breakthrough is paramount, and a realistic load resistance estimate is all important. Given that the data in Fig. 5 of the authors' paper do not ''visually demonstrate the invalidity of Sodhi's claim that there is no size effect,'' one would intuitively favor a more conservative approach in the latter instance.

Conclusion: A fundamental requirement of a Bažant-type size effect analysis is the stable and self-similar growth of crack-front contiguous cohesive-type process zones. Such behavior is deemed implausible for the problem at hand. While a size effect may occur for thick ice sheets, it is unlikely to be significant for ice thicknesses less than 1 m.

APPENDIX. REFERENCES

DeFranco, S. J., and Dempsey, J. P. (1994). ''Crack propagation and fracture resistance in saline ice.'' *J. Glaciology*, 40, 451–462.

Dundurs, J. (1975). ''Properties of elastic bodies in contact.'' *The mechanics of the contact between deformable bodies*, A. D. de Pater and J. J. Kalker, eds., Delft University Press, Delft, The Netherlands.

Discussion by Devinder S. Sodhi[4]

In their papers, the authors arrive at the conclusion there is a size effect on the failure load of floating ice sheets for ice thicknesses greater than 0.2 m. However, the results of their analysis are only useful if the assumptions made in their anal-

[a]December 1998, Vol. 124, No. 12, by Zdeněk P. Bažant and Jang Jay H. Kim (Papers 14531 and 17980).

[3]Dept. of Civ. and Envir. Engrg., Clarkson Univ., Potsdam, NY 13699-5710. E-mail: john@clarkson.edu

[4]U.S. Army Cold Regions Res. and Engrg. Lab., 72 Lyme Rd., Hanover, NH 03755-1209. E-mail: dsodhi@crrel.usace.army.mil

ysis correspond to the real situation during vertical loading and breakthrough failure of floating ice sheets.

PART I

The process of a gradually increasing axisymmetric load on a floating ice sheet results in the following sequence of events: (1) elastic deformations; (2) formation of radial cracks; (3) wedging of radially cracked segments of ice sheets; (4) formation of many circumferential cracks; and (5) breakthrough due to large deformation or brittle failure of ice. If the loading rate is low, we also need to consider creep deformation of ice along with elastic deformation. During field tests, it is often difficult to observe their formation because of snow cover. During small-scale tests, the formation of radial cracks is a very short-time event. They propagate to a length of about 2–3 times the characteristic length and arrest. After the formation of radial cracks, compressive stresses in the top part of the ice sheet support the load because of the wedging or dome effect. The compressive stresses cause creep deformation of ice, resulting in further deformation.

The results of linear elastic fracture mechanics analysis are not immediately relevant to the propagation of cracks in a creeping material. The results of Slepyan (1990) and Bazant and Li (1994) are particularly flawed, because the interference between segments during elastic deflections of wedge-shaped beams was ignored. Dempsey et al. (1995) presented a formulation of plates having radial cracks with closure. Bazant et al. (1995) and Bazant and Kim (1998) consider closure of part-through cracks, and the failure criterion is the formation of the first circumferential crack. They did not consider the creep deformation of ice, nor did they consider the formation of multiple circumferential cracks, which have been observed in small-scale and full-scale tests. The authors arrive at a result that the dependence of breakthrough load P_f is proportional to $h^{3/2}$ using the results of field tests by Frankenstein (1963, 1968) and Lichtenberger et al. (1974). Those field tests were conducted by loading an ice sheet at a constant rate, and some of these tests lasted for hours. Therefore, it is not reasonable to use the results of those field tests to support the conjecture that fracture, while ignoring creep, gives the size effect $P_f \propto h^{3/2}$ for ice thickness greater than 0.2 m. Their criterion that an ice sheet fails when the first circumferential crack forms is also not correct, because many circumferential cracks form around the area of load application before final breakthrough takes place.

PART II

In their analysis, the authors considered a hole of radius equal to 10% of the characteristic length and assumed the load to be distributed at the periphery of the hole. Because there is considerable deformation of material in the area close to the center, the conclusion they have reached may not be totally correct.

On page 1320, they state that ''Frankenstein made extensive observations on lake ice, which can be assumed to behave similarly as sea ice.'' Yet they criticized Sodhi (1995b, 1998) at the bottom of page 1321 by saying that ''a second questionable aspect of Sodhi's (1995a,b) evaluation of test data is that he correlated in the same diagram the test results from different test series while implying the same ice properties. However, the ice properties were most likely quite different.'' Nevertheless, the authors plot the data from tests with freshwater and sea ice in Figs. 5(c and d).

On page 1321, the authors state: ''In view of the high scatter and limited size range of the available data, it cannot be claimed, however, that results actually prove the present theory.'' Yet the authors state on the bottom of the same page: ''Nevertheless, all the plots in Fig. 5 visually demonstrate the invalidity of Sodhi's claim that there is no size effect.'' In Figs. 5(a and b) of the paper, the authors have not really proven the existence of a size effect by fitting curves through three sets of data having high scatter and a narrow range of ice thickness.

In Fig. 6, results of small-scale and full-scale tests are plotted in terms of ice thickness versus failure load. This figure includes the data from ICEX-93 tests, in which ice penetration forces were measured during uplifting and breakthrough of floating ice sheets by two submarines (Dane 1993; Sodhi 1998). A line $P_f = 1{,}934\ h^2$ (where P_f is in kN and h is in m), obtained from the results of small-scale tests, passes through plots of full-scale data, which have considerable scatter. Because this line passes through the middle of the full-scale data, the discusser concluded that there is no size effect for ice thickness up to 2 m (Sodhi 1995b, 1998). Compilation of field data by Gold (1971) also supports failure load being proportional to the square of the ice thickness. Accepting the authors' conclusion that there is no size effect for ice thickness less than 0.2 m, the discusser has plotted a line representing $P_f \propto h^{3/2}$ in Fig. 6 from a point on the line ($P_f = 1{,}934\ h^2$), where ice thickness is equal to 0.2 m. This line does not fit the data obtained from full-scale tests on freshwater and sea ice.

The authors raise a point in the paper that the properties of

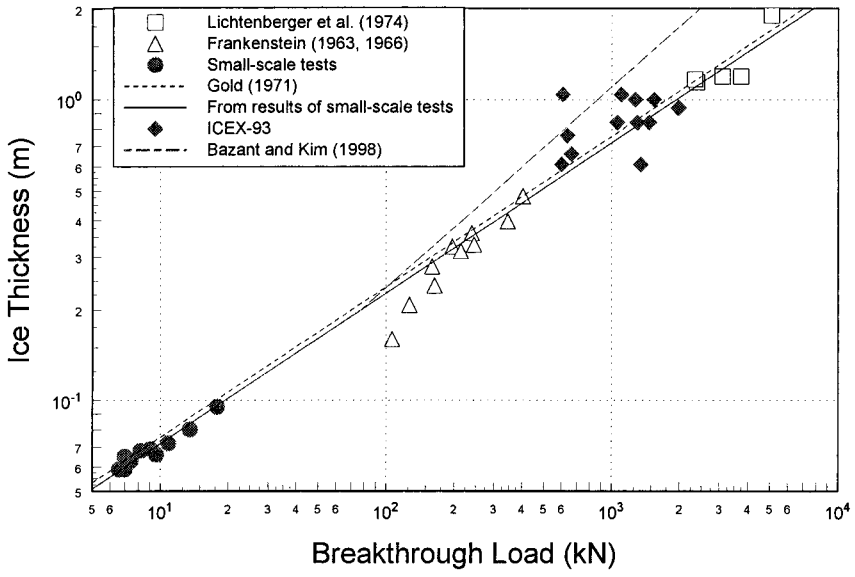

FIG. 6. Ice Thickness versus Breakthrough Load of Floating Ice Sheets

freshwater and sea ice may influence the failure load. However, the discusser considered creep properties of freshwater and saline ice and did not find much deviation between a line ($P_f \propto h^2$) and the estimated failure loads (Sodhi 1995a). The dependence of failure loads on salinity of ice appears to be a secondary effect, but its dependence on h^2 is supported by the strength failure criterion (Bazant 1993) because of creep deformation during wedging action.

On page 1322, the authors state: ''Sea ice exhibits creep, and the effective fracture energy as well as the strength depends on the rate of crack growth.'' Analysis of this problem incorporating creep will require abandoning LEFM, on which they base their present conclusions.

APPENDIX. REFERENCES

Dane, A. (1993). ''Ice station X.'' *Popular Mech.*, 170(11), 30–34, 132.

Gold, L. W. (1971). ''Use of ice covers for transportation.'' *Can. Geotech. J.*, Ottawa, Canada, 8, 170–181.

Sodhi, D. S. (1998). ''Vertical penetration of floating ice sheets.'' *Int. J. Solids and Struct.*, 35(31–32), 4275–4294.

Closure by Zdeněk P. Bažant,[5] Fellow, ASCE, and Jang Jay H. Kim[6]

DEMPSEY'S DISCUSSION

Dempsey's thoughtful and stimulating discussion is deeply appreciated by the writers. Citing certain simplifications made in the paper and revoking his own analytical solution, Dempsey states that dynamic fracture propagation instabilities may cause the size effect to be significant only for rather thick ice plates, thicker than about 1 m. Dempsey et al.'s (1995) elegant analytical solution, however, rested on even stronger simplifications, which render his conclusion about the lack of size effect for not too thick plates unjustified.

Dempsey assumes the cracks to reach through the full ice thickness, which implies the stress intensity factor K_I at the boundary of the crack closure zone (contact zone) is zero. Consequently, there is no dissipative mechanism at all in Dempsey et al.'s solution. No energy is dissipated by the fracture process as modeled. Despite the possibility of dynamic instabilities described by Dempsey, this seems to be a severe simplification.

Another drastic simplification in Dempsey et al.'s (1995) solution is that the depth profile of the open crack along the radial coordinate is assumed to be uniform from the load point up to the tip of the radial crack, with a discontinuous jump at the tip. The numerical solution in the paper, by contrast, revealed that the depth of the opened crack varies strongly with the radial coordinate and, at the radial crack front, approaches zero continuously.

The solution in the paper has proven that a static loading process cannot produce radial cracks that cut through the full ice thickness. Dempsey argues that full-through cracks are produced by dynamic instabilities, after which the crack partially closes because of arching (or dome) action. To support his view, he cites the fact that, in field experiments, the top surface of ice was seen to whiten along the radial cracks. This observation, however, does not proves Dempsey's point, in the writers' opinion. Cracks actually reaching the surface were not observed in the field. The observed whitening of the top surface of the ice was more likely caused by distributed cracking, which occurs in the fracture process zone of sea ice. The correct interpretation should be that the fracture process zone reaches close to the top surface. But this is not incompatible with the notion that the equivalent LEFM cracks reach to about 85% of ice thickness, as found in the paper.

Dempsey is not right in stating that ''the issue of crack growth stability ... was bypassed by Bažant and Kim.'' Because, as shown in the paper, the vertical load increases with an increasing displacement, it is immediately clear that the solution obtained is stable (which means that this is a fracture problem of positive geometry, in fracture mechanics terminology). Contrary to Dempsey's comment, the solution is stable regardless of whether the radial crack length or the load-point displacement is controlled. The purpose of using in computations the crack length control instead of the displacement control was not to achieve stability of the actual response but merely to improve the convergence of iterations (or ensure stability of the numerical algorithm).

In principle, of course, it should not be ruled out that removal of some simplifying assumptions may lead to a significantly different solution exhibiting dynamic instabilities. There exist two possible sources of the dynamic instabilities emphasized by Dempsey: (1) strong inhomogeneity of sea ice; and (2) three-dimensionality of fracture propagation near the radial crack front, alluded to by Dempsey, which is undescribable by the assumed vertical propagation along an infinitesimal strip.

At the critical state of the stability limit, a structure is at the limit of static response (equilibrium). When stability is lost, the response becomes dynamic (i.e., there must be inertia forces to satisfy D'Alembert equations of dynamic equilibrium). Since the static solution for a homogeneous ice plate is stable, the only possible cause of unstable crack jumps (inevitably dynamic) is periodic inhomogeneity of ice properties. The value of fracture toughness K_c, considered constant in the paper, actually fluctuates randomly along the crack path (with some dominant wavelength l_c, representing the dominant spectral component of the random process of K_c as a function of crack path length).

In crack path segments in which K_c is decreasing fast enough, crack propagation may become unstable, dynamic. But it must be a snap-through instability, with a jump to a new stable equilibrium state, which must occur in the next crack path segment in which K_c is growing, constant, or not decreasing fast enough. Since every material is inhomogeneous, such instabilities occur in all fracture. They get manifested by acoustic emissions. Yet static LEFM still provides the correct approximation on the macroscale.

One might think that the rate of energy to form the fracture should be equal to the rate of stored energy release minus the rate of the energy radiated by acoustic waves. But the energy of acoustic emissions in ice may surely be considered negligible compared with the total energy needed to form the cracks. In concrete, for example, the acoustic emissions, due to snap-throughs at each fluctuation of fracture toughness caused by aggregate pieces, are as strong as in ice, yet it is generally accepted that the energy they radiate is insignificant compared with the energy required for concrete fracture. Otherwise, static fracture analysis of concrete would be impossible. Besides, it would actually be incorrect to subtract the energy of acoustic emissions, because it is never subtracted during the measurement of fracture energy. So the fracture energy value used in fracture calculations already includes the energy of acoustic emissions.

Dempsey apparently believes that the typical length of the segments of decreasing K_c along the crack's path (or the dominant spectral wavelength l_c, or the length of crack front jumps) is not microscopic, negligibly short compared with the radial crack length, but relatively long. But unless this length were

[5]Walter P. Murphy Prof. of Civ. Engrg. and Mat. Sci., Northwestern Univ., Evanston, IL 60208.

[6]Formerly, Grad. Res. Asst., Northwestern Univ., Evanston, IL.

comparable to the entire radial crack length (i.e., unless almost the whole radial crack forms dynamically), a static fracture analysis must still provide at least an approximate overall description, correct in the energetic sense.

Static approximations to dynamic instability in the form of a snap-through from one equilibrium state (the initial uncracked state) to another equilibrium state (the full-through crack with partial closure) must generally satisfy Maxwell's condition of energy equivalence (whose classical example is the Maxwell line through the instability in the van der Waals pressure-volume diagram for the vapor-liquid phase transition). But even if a dynamic snap-through from an uncracked state to a full-through crack followed by a partial crack closure were the actual fracture mechanism, Dempsey et al.'s solution does not appear to be energy consistent.

The solution in the paper, on the other hand, is energy consistent. Unlike Dempsey et al.'s solution, it guarantees the rate of release of the stored strain energy and gravitational energy of sea water to be equal to the rate of energy needed to form the radial cracks in ice, corresponding to the given value of the fracture energy of ice. Thus, the condition of overall energy balance is satisfied.

In view of the foregoing considerations, as well as the fact that no solution with a dynamic instability has yet been presented, Dempsey's concern about the dynamic instabilities appears exaggerated. It is clear from the solution in the paper that, under the assumptions made, the load is continuously increasing with the crack length as well as with the load-point displacement. This guarantees continuous stability up to the moment of formation of the circumferential cracks, provided that the ice is treated as homogeneous.

The second suspected source of error, the three-dimensionality, is reflected in Dempsey et al.'s solution to a lesser degree than by the solution in the paper. Dempsey et al.'s assumption that the depth of open crack along the radial crack is uniform, with a sudden jump to zero at the radial crack front (a place where the dynamic crack jumps would have to take place), is a rather severe simplification of a plausible fracture shape. In the paper, the open crack depth is variable and at the radial crack front approaches zero without any discontinuity. The depth variation is found to be quite significant. Therefore, the deviation from the actual three-dimensional behavior is evidently greater for Dempsey et al.'s solution.

It is strange that, while questioning the existence of size effect except in very thick plates, Dempsey ignores the evidence given by Fig. 5 in Part II of the paper. That figure shows the results of three field tests, and each of them clearly shows, despite high scatter, that a strong size effect is present even for a size range beginning with 0.1 m.

In conclusion, the writers remain convinced that the simplifications made in the fracture and size effect analysis of the paper were not unreasonable and that the numerical solution presented, with all its approximations, ought to be more realistic than the analytical solution of Dempsey et al., ingenious and elegant though it may be. In particular, the writers do not agree with Dempsey that a static analysis leading to ''stable and self-similar growth'' would be implausible. Simplified though the analysis in the paper obviously is, it nevertheless appears to be a reasonable simplification.

SODHI'S DISCUSSION

Sodhi has made some interesting and thought-provoking points. However, his severe criticism is unconvincing and, in the writers' opinion, invalid.

It is true that the neglect of radial crack closures in Slepyan (1990) and Bažant and Li (1994) was an oversimplification, but these early studies, judged as ''particularly flawed'' by Sodhi, represented necessary steps in the evolution toward a realistic fracture analysis and clarified some important aspects of the scaling problem. Prior to Dempsey et al. (1995) and Bažant et al. (1995), no fracture studies of ice plate penetration took the crack closures with the inherent dome effect into account (some limit analysis studies did, but to treat ice as a plastic material without softening damage is a much more serious ''flaw,'' in the writers' opinion).

There is no dispute that certain simplifying assumptions were made in the paper, but the writers believe them to be reasonable and sufficiently realistic. One simplification was the neglect of creep, which is repeatedly reproached by Sodhi. However, assuming that creep would not mitigate the size effect is not baseless.

There used to be a widespread intuitive misconception that the influence of creep is like that of plasticity, which tends to increase the process zone size, thereby making the response less brittle and the size effect weaker. But the influences of creep and plasticity are very different.

The influence of creep on scaling of brittle failures of concrete, which is doubtless quite similar from the mechanics viewpoint (albeit different in physical origin), was studied in depth at Northwestern University, along with the effect of the crack propagation velocity; see, e.g., Bažant and Gettu (1992); Bažant et al. (1993); Bažant and Planas (1998); and especially Bažant and Li (1997) and Li and Bažant (1997). The conclusion from these studies, backed by extensive fracture testing of concrete and rock at very different rates, is that, unless creep actually prevents crack formation, creep in the material always makes the size effect due to cracks stronger. In the logarithmic size effect plot of nominal strength versus structure size, it causes a shift to the right, toward the LEFM asymptote.

In light of these studies, Sodhi's claim (in his last paragraph) that ''incorporating creep will require abandoning an LEFM approach'' must be seen as erroneous. The opposite is in fact true: The slower the loading (or the longer its duration), the closer to LEFM is the size effect in a cracked structure. The physical reason, clarified by numerical solutions of stress profiles with a rate-dependent cohesive crack model (Li and Bažant 1997), is that the highest stresses in the fracture process zone at the crack front get relaxed by creep, which tends to reduce the effective length of the fracture process zone. The shorter the process zone, the higher the brittleness of response is and the shorter the size effect. This explains why experiments on notched concrete specimens consistently show the size effect to be stronger at a slower loading (Bažant and Planas 1998). It is highly probable that the same will be verified for ice, once size effect tests at very different loading rates are carried out.

From the aforementioned studies, it thus transpires that, in order to take the influence of creep on the size effect approximately into account, one does not need to abandon equivalent LEFM, as claimed by Sodhi. It suffices, in the case of very slow loading, to reduce the value of fracture energy (or fracture toughness) and decrease the effective length c_f of the fracture process zone. Even these adjustments, however, are important only when loading durations differing by several orders of magnitude are considered, which is not the case for the ice penetration tests cited by Sodhi.

Sodhi also states that considering the load to be applied along the circumference of a hole of a radius of about 10% of the characteristic length must have caused the results not to be ''totally correct,'' apparently meaning not totally representative of the idealized case of a concentrated load applied at a point. However, the conclusions ought to be essentially correct. Fracture is at a maximum load driven by the global energy release from the ice plate—sea water system and is not very sensitive to local disturbances near the load application point, where reach is limited according to Saint-Venant principle.

Sodhi's comments in the second paragraph of Part II are taken out of context and result from a misunderstanding of the criticism in the original paper of Sodhi's previous way of handling the available data sets. In Figs. 5(c and d) of the paper, cited by Sodhi, the coordinates are not the actual thickness D and nominal strength σ_N but their relative values, which are normalized by the values of $\lambda_0 l_0$ and Bf_t only *after* these values have already been determined for each data set separately. The two plots were presented in the paper merely for visual demonstration; they were not used for actually identifying the material parameters from the test data. On the other hand, in his previous works cited from the paper, and again in his present discussion, Sodhi plots the data from different data sets in the same plot and actually uses regression in this plot to determine the parameter values. The criticism of such a procedure stated in detail in the paper is valid.

Since the relation of the ice properties in various data sets is not known a priori, an arbitrary vertical or horizontal shift (in log σ_N) of the group of data points from one data set against that from another data set is allowed and must be considered. Just by choosing a suitable vertical or horizontal shift of the data groups, any desired conclusion can thus be obtained—the presence of a strong size effect, or the absence of any size effect (in Sodhi's case). Nothing is thus proven by Sodhi's plot. This is the salient point criticized in the paper.

The kind of plot shown in Fig. 6 and discussed in Sodhi's fourth paragraph, Part II, is misleading for two reasons: (1) as known from Buckingham's theorem of dimensional analysis, general physical laws are correct only if they can be written in a dimensionless form; and (2) the breakthrough load $P_{\max}$ must obviously depend on ice strength f_t'. To achieve a dimensionless coordinate, the breakthrough load in Fig. 6 must be divided by $f_t' h^2$, h being the ice thickness (a division by f_t' amounts to a horizontal shift in the logarithmic scale). But then it is not a priori clear how the f_t' values for different data sets relate to each other, because they have not been separately identified in advance.

Consequently, the relative horizontal positions of the groups of circles, triangles, diamonds, and squares in Fig. 6 must be considered as undetermined in advance. This implies that Sodhi's plot in Fig. 6 can be valid only for one kind of ice, not for different kinds simultaneously. Arbitrary vertical shifts of one data group against another, due to unknown differences in f_t', would have to be considered in Fig. 6 if the breakthrough load were normalized by the ice strength. [Here the shifts are not vertical, as considered in the paper, but rather horizontal, because Sodhi for some reason inverts the coordinates; the ice thickness (normalized) would normally be the coordinate and the breakthrough load (normalized) the ordinate.]

The ice thickness h in Fig. 6 should of course also be normalized to yield a dimensionless coordinate. One way to do that might be to adopt as the ordinate the dimensionless parameter $h\rho_w/f_t'$, where ρ_w is the specific weight of water (of dimension N/m^3). In that case, the vertical and horizontal shifts in Fig. 6 are the same and thus the plot looks the same after the shifts. But ρ_w/f_t' is not the only possible normalizing factor for h and is in fact not the most reasonable one.

If fracture plays any role, then either the characteristic length l_0 of the cohesive crack model or the effective length of the fracture process zone in the sense of equivalent LEFM must somehow appear in the solution. So the ice thickness h should correctly be normalized by l_0. In other words, the ordinate h in Fig. 6 should be replaced by the relative thickness h/l_0. With this reasonable normalization of h, the arbitrariness of the horizontal shifts pointed out in the previous paragraph remains. Ignoring this kind of normalization of h, which is implicit to Sodhi's approach, is tantamount to assuming a priori that fracture mechanics plays no role in the problem and that there is no size effect. Given that such a hypothesis is implied, Sodhi's use of Fig. 6 to dismiss the size effect appears to be a circular argument.

Still another noteworthy point, already made in the paper, is that the coordinate of the size effect plots should not be the load P but the nominal strength $\sigma_N = P/h^2$. The case of no size effect then corresponds to a horizontal line. The plot in terms of P superimposes on the size effect the underlying proportionality of P to h^2 corresponding to the strength theory, which does not represent a size effect as generally understood. This obscures the size effect, as demonstrated by Figs. 4(b and c) of the paper. Sodhi does not question this demonstration, yet he persists in his discussion in plotting the size effect again in terms of P rather than σ_N.

APPENDIX. REFERENCES

Bažant, Z. P., and Gettu, R. (1992). "Rate effects and load relaxation: static fracture of concrete." *ACI Mat. J.*, 89(5), 456–468.

Bažant, Z. P., Bai, S.-P., and Gettu, R. (1993). "Fracture of rock: effect of loading rate." *Engrg. Fracture Mech.*, 45(3), 393–398.

Bažant, Z. P., and Li, Y.-N. (1997a). "Cohesive crack with rate-dependent opening and viscoelasticity. I: Mathematical model and scaling." *Int. J. Fracture*, 86(3), 247–265.

Li, Y.-N., and Bažant, Z. P. (1997b). "Cohesive crack with rate-dependent opening and viscoelasticity. II: Numerical algorithm, behavior, and size effect." *Int. J. Fracture*, 86(3), 267–288.